blood®
Regular Article

LYMPHOID NEOPLASIA

Integrative genomic analysis of pediatric T-cell lymphoblastic lymphoma reveals candidates of clinical significance

Tasneem Khanam,[1] Sarah Sandmann,[2] Jochen Seggewiss,[3] Charlotte Ruether,[1] Martin Zimmermann,[4] Allison B. Norvil,[5] Christoph Bartenhagen,[2,6] Gerrit Randau,[1] Stephanie Mueller,[1] Heidi Herbrueggen,[1] Per Hoffmann,[7] Stefan Herms,[7] Lanying Wei,[2] Marius Woeste,[2] Christian Wuensch,[2] Humaira Gowher,[5] Ilske Oschlies,[8] Wolfram Klapper,[8] Wilhelm Woessmann,[9] Martin Dugas,[2] and Birgit Burkhardt[1]

[1]Department of Paediatric Hematology and Oncology, University Hospital Muenster, Muenster, Germany; [2]Institute of Medical Informatics and [3]Institute of Human Genetics, Muenster University, Muenster, Germany; [4]Department of Pediatric Hematology and Oncology, Hannover Medical School, Hannover, Germany; [5]Department of Biochemistry, Purdue University, West Lafayette, IN; [6]Department of Experimental Pediatric Oncology, University Children's Hospital, Cologne, Germany; [7]Institute of Human Genetics, Department of Genomics, Life and Brain Center, University of Bonn, Bonn, Germany; [8]Hematopathology Section, Department of Pathology, University Hospital Schleswig-Holstein Campus Kiel, Kiel, Germany; and [9]Department of Pediatric Hematology and Oncology, University Medical Center Hamburg-Eppendorf, Hamburg, Germany

KEY POINTS

- **NOTCH/PI3K-AKT signaling axis and cell cycle regulators are the key players that drive T-LBL.**
- **Mutations in *KMT2D*, an epigenetic modifier, are associated with poor prognosis in T-LBL.**

T-cell lymphoblastic lymphoma (T-LBL) is a heterogeneous malignancy of lymphoblasts committed to T-cell lineage. The dismal outcomes (15%-30%) after T-LBL relapse warrant establishing risk-based treatment. To our knowledge, this study presents the first comprehensive, systematic, integrated, genome-wide analysis including relapsed cases that identifies molecular markers of prognostic relevance for T-LBL. *NOTCH1* was identified as the putative driver for T-LBL. An activated NOTCH/PI3K-AKT signaling axis and alterations in cell cycle regulators constitute the core oncogenic program for T-LBL. Mutated *KMT2D* was identified as a prognostic marker. The cumulative incidence of relapse was 47% ± 17% in patients with *KMT2D* mutations, compared with 14% ± 3% in wild-type *KMT2D*. Structural analysis of the mutated domains of *KMT2D* revealed a plausible impact on structure and functional consequences. These findings provide new insights into the pathogenesis of T-LBL, including high translational potential. The ongoing LBL 2018 trial (www.clinicaltrials.gov #NCT04043494) allows for prospective validation and subsequent fine tuning of the stratification criteria for T-LBL risk groups to improve survival of pediatric patients. (*Blood*. 2021;137(17):2347-2359)

Introduction

T-cell lymphoblastic lymphoma (T-LBL) represents the second most frequent subtype of non-Hodgkin lymphoma (NHL) in children and adolescents. T-LBL displays a large overlap with acute T-cell lymphoblastic leukemia (T-ALL) in morphological, clinical, and immune-phenotypic features.[1,2] Hence, it is often debated whether T-LBL and T-ALL are different entities or represent manifestations of the same disease.[3] T-LBL presumably develops from a multistep process wherein aberrant genetic and epigenetic alterations result in increased cell proliferation, survival, self-renewal, and arrest of differentiation of immature T-cell progenitors.[4] Gain-of-function mutations in *NOTCH1* have been extensively reported and characterized in T-ALL,[5-15] and recent studies have reported a similar frequency of *NOTCH1* mutations in T-LBL.[1,16-18] Loss-of-function (LOF) mutations in *PTEN* result in constitutive activation of PI3K-AKT in T-ALL[19] and T-LBL.[18] Interestingly, cross talk between NOTCH and PI3K-AKT signaling is reported in T-ALL. Blocking activity of *NOTCH1* results in upregulation of *PTEN* and inhibition of PI3K-AKT pathway.[19,20] Most of the identified mutations for pediatric T-ALL can be assigned to NOTCH, PI3K/AKT/mTOR, and JAK/STAT signaling pathways and epigenetic modifiers.[21-23] *BCL11b* is associated with improved overall survival in adult T-ALL, but not in pediatric T-ALL.[24,25] So far, *BCL11b* has not been investigated in T-LBL. Furthermore, chromosome 9p deletions have been identified in both T-LBL and T-ALL, although they were not associated with prognostic relevance.[1,26]

Epigenetic modifications play an important role in establishing T-cell identity.[27] *KMT2D* is frequently mutated in NHL and other cancers.[28-30] LOF mutations in *KMT2C* and *KMT2D* promote tumorigenesis by dysregulation of enhancer- and superenhancer-related genes.[31-33] The precise order of acquiring genetic and epigenetic lesions during the initiation of T-LBL is largely unknown, because T-LBL molecular data are sparse. Genome-wide information is lacking except for limited reports of

whole-exome sequencing (WES),[34,35] and there are few studies of gene expression profiles,[1,2] methylation profiles, and copy number alterations (CNAs).[1,36] Therefore, little is known about markers with prognostic relevance for T-LBL.[16-18,34,37] The lack of valid prognostic markers and the poor chance of surviving relapse underline the medical need to learn more about the pathogenesis and the molecular characteristics in T-LBL. The key findings from the current analysis include identification of recurrent genetic alterations, additional potential hotspots in previously identified molecular markers, altered pathways, and potential prognostic markers for T-LBL.

Patients and methods

Patient samples

From 1995 through 2018, 668 pediatric and adolescent patients with T-LBL were registered in the NHL-BFM (non-Hodgkin lymphoma-Berlin-Frankfurt-Muenster) study center. Informed consent was obtained from parents or guardians. Patients were treated uniformly according to NHL-BFM treatment protocol for LBL, as described previously.[38] Clinical data for patient characteristics, diagnostics, treatment, and outcome were obtained from the clinical trial databases. For the current study, lymphoma samples from 131 patients referred to as the "extended cohort" were included, of which 127 samples were evaluable (supplemental Table 1; supplemental Figure 1, available on the *Blood* Web site). In addition, corresponding germline samples from 29 patients were included.

WES and targeted sequencing

WES was performed on a "limited cohort" of 16 patients with T-LBL, including 10 paired samples (10 germline and 10 diagnostic/primary samples), and 6 triplet samples, including corresponding relapse samples (6 germline, 6 primary, and 6 relapse). "Primary samples" refers to those collected at the time of diagnosis before the start of therapy from patients who did or did not experience relapse; "relapse samples" refers to samples collected from patients after relapse but before the commencement of relapse therapy. One of the samples was excluded from the WES analysis due to tumor cell content in the corresponding germline sample. WES was performed (mean depth, ~300×) with the Sureselect XT Human All Exon V6+COSMIC panel. The WES data were validated by high coverage, targeted sequencing of ~5000× for germline and ~6000× (with duplicates) for primary and relapse samples with a capture-based technique from Agilent Technologies. The targeted panel for T-LBL was designed with 76 to 80 genes, the probes were designed for complete coding regions of the genes, except in the case of 5 large genes, for which probes were included only for specific exons (supplemental Table 2). Further details are provided in the supplemental Materials and Methods.

SNP arrays and methylation arrays

Single nucleotide polymorphism (SNP) analyses were performed on arrays from Infinium Omni2.5Exome-8 v1.3 for the limited cohort and on arrays from Infinium Omni2.5Exome-8 v1.4 for the *TP53*-mutated samples (n = 6; variant allele frequency [VAF] cutoff, 1). Methylation analyses were performed with arrays from the Infinium MethylationEPIC BeadChip Kit[39] on samples from the limited cohort. Data were analyzed by Illumina GenomeStudio 2.0.3. All samples passed the quality control quality control filters with genotyping rates ≥0.99 and no conspicuous control probes. Copy number variations [CNVs] were called by using cnvPartition 3.2.0, with a minimum probe count of 10. Output from GenomeStudio was manually inspected in comparison with the called CNVs. Details of the analysis of the methylation arrays and genotyping are provided in the supplemental Materials and methods.

Multiplex ligation-dependent probe amplification

LOH6q analysis was performed with SALSA multiplex ligation-dependent probe amplification (MLPA) P200 Reference-1 in combination with custom-made probes and the SALSA MLPA EK1 reagent kit-FAM (MRC Holland, Amsterdam, The Netherlands), as described by Rohde et al.[40] The SALSA MLPA probemix P383T-A2 T-ALL (MRC-Holland, The Netherlands) was used to screen the *PTEN* deletions. Details are provided in the supplemental Materials and methods.

Absence of biallelic TCR-γ deletion analysis

Single-tube multiplex T-cell receptor γ chain gene (TRG) polymerase chain reaction was performed as described by Derrieux et al.[41] Details of the analysis are provided in the supplemental Materials and methods.

Statistical analysis

For the analysis of targeted sequencing data, only mutations in primary samples from both nonrelapse and relapse cases, with a VAF cutoff of 10% were included. Synonymous mutations in *NOTCH1* and *FBXW7* were excluded. To maintain consistency with earlier published data,[16,17] only data for mutations of *NOTCH1* and *FBXW7* in the reported hotspots were included. In addition, analysis was performed that included all the mutations of *NOTCH1* and *FBXW7*. Statistical analysis was also performed as described previously[17] for CNAs for genes included in MLPA probemix P383T-A2 T-ALL. Cumulative incidence functions for relapse (CIR) were constructed by the method of Kalbfleisch and Prentice and compared by using Gray's test. Differences in distribution of individual parameters among patient subsets were analyzed by χ^2 test or Fisher's exact test. Multivariate analysis of the CIR was performed according to the Fine and Gray model.[42]

Simulation of structures and modeling of the mutations in *KMT2D*

The primary amino acid sequence of *KMT2D* was analyzed by the VSL2 (VSL2-M1) predictor tool to predict disordered regions.[43] Phyre2[44] was used in intensive mode to model the PHD_7, FYR, and SET domains and also structural changes after the mutated residues were inserted. The structures of the FYRN and FYRC motifs of *KMT2D* were modeled using the crystal structure of *TBRG1*,[45] and zinc molecules (Zn^{2+}) were modeled into the structure using PyMOL. The crystal structure of the SET domain of *KMT2D* (PDB: 4Z4P)[46] was used to model the mutation identified in the SET domain.

Results

Genome-wide screening for recurrent genetic and epigenetic alterations in T-LBL

WES revealed 1168 somatic mutations, of which 70% were nonsynonymous and included 49 indels. The majority of the

samples (18 of 20) demonstrated a low tumor mutational burden of 0.39/Mb (supplemental Table 3), except for 2 hypermutated relapse samples (TR14 and TR15) with a mutation rate of 7.93 and 2.89/Mb, respectively. Both cases featured mutations in *MLH1* (Figure 1A; supplemental Figure 2) involved in mismatch repair.[47] *NOTCH1* (73%) and *FBXW7* (33%) were the most recurrently mutated genes. *NOTCH1* was identified as the putative driver gene (supplemental Table 4) by MutSigCV ($P = .0028$).[48] About 27% of genes from the published WES data[34] overlapped with those in the current data. Bioinformatic analysis[49] revealed altered key pathways, namely the NOTCH, JAK-STAT, PI3K-AKT, Ras, and P53 signaling pathways, and also cell-cycle regulators, epigenetic modifiers, and transcription factors involved in T-cell development that presumably drive T-LBL. Besides somatic mutations in *NOTCH1* and *FBXW7*, hypermethylation of *NCOR2*, a regulator of NOTCH signaling,[50] and of *FOXP1*, a key transcriptional regulator for T cells,[51] was observed in comparison with their corresponding germline samples (Figure 1B-C). Although no major difference in methylation was observed between primary and relapse samples or between primary samples from patients who relapsed (primary-relapse$^+$) and those who did not (primary-relapse$^-$), a small number of genes were hypomethylated in primary-relapse$^+$ cases in comparison with primary-relapse$^-$ (supplemental Figure 3A-C). Interestingly, some of these genes, such as *SOX2OT*, *PEPD*, and *WBSCR17*, were reportedly involved in tumor progression, aggressive phenotype, and treatment resistance in several cancers.[52-54] Frequent deletions in the chromosome 9p region, including the CDKN2A/2B locus encoding *p16/INK4A* and *p14/ARF* tumor suppressors involved in cell cycle regulation, were identified in primary-relapse$^-$ cases, and amplifications in chromosome 8 were seen in primary-relapse$^+$ cases and in their corresponding relapse samples. Four of 16 cases revealed deletions in chromosome 17 and 1 of them also revealed amplification in chromosome 17 (Figure 1D). LOH for *TP53* was identified in only 1 case, in both the primary sample and in the corresponding relapse sample (TP16 and TR16). In *STAT5B*, a duplication event in 1 of the primary samples (TP15) and LOH in the corresponding relapse sample (TR15) were confirmed. Results from 16 SNP arrays were validated alterations: deletions in *CDKN2A/2B* (n = 16), *LEF1* (n = 3), *MLLT3* (n = 3), *MTAP* (n = 2), *SUZ12* (n = 2), and *NF1* (n = 1) and gains in *EZH2* (n = 2), *CASP8AP2* (n = 1) and *MYB* (n = 1) were confirmed.

Mutational spectrum and recurrently altered pathways of T-LBL

Integrated analysis was performed for the extended cohort including targeted sequencing (Figure 2, VAF cutoff, >10%; supplemental Figure 2, VAF cutoff, >1%) of a panel of 76 to 80 genes, validation of CNAs, and analysis of additional markers. Constitutive activation of NOTCH signaling (68%) along with deletion of the *CDKN2A* (75%) and *CDKN2B* (61%) locus in the chromosome 9p region, as previously reported for T-LBL[26] and T-ALL,[4,21] emerged as main oncogenic lesions in T-LBL. *NOTCH1* (63%) and *FBXW7* (25%) mutations were identified at known hotspots[7,16,17] and were analogous to hotspots in T-ALL.[5,15,55] Additional somatic mutations were identified in other exons besides the reported hotspots both in *NOTCH1* and *FBXW7* (supplemental Figure 4A-C). Interestingly, another candidate, *NOTCH3* from the NOTCH signaling pathway, was mutated in 8% of cases. Four of 10 *NOTCH3*^{mut}s cooccurred with *NOTCH1*^{mut} mutations. *BCL11b* mutated in 9% of cases in our current analysis, similar to its mutation rate in pediatric T-ALL (supplemental Figure 5A).[25]

PI3K-AKT was identified as the second most affected pathway. Mutations identified in *PTEN* (15%), a negative regulator of PI3K-AKT pathway, and in *PIK*3CA (7%) were slightly higher than previously reported (6%)[18] and could result in activation of the PI3K-AKT pathway.[56,57] Interestingly, all *PTEN* mutations were nonsynonymous and mostly located at the hotspot reported in T-ALL and T-LBL,[56-58] with a few in other exons (supplemental Figure 5B). In addition, deletions in *PTEN* (*PTEN*del) were identified in 19% of cases, and of those, 9 cases displayed both mutations and deletions. In *PIK3CA*, mutations were identified at hotspots in exons 10 and 21, as reported earlier,[18] and in other exons (namely, exons 1, 8, and 18). The JAK-STAT pathway was identified as the third most affected pathway. *STAT5B*, a mutation often reported to be associated with an inferior response, mutated in 6% of the cases.[59,60] Some of the mutations identified in *STAT5B*, *JAK3*, and *IL7R* in the current study reportedly have an activating effect on the JAK-STAT pathway or IL7R signaling in T-ALL and other cancers.[59,61-66] Besides the activating mutation N642H,[59,61] G698V was identified as a novel mutation in *STAT5B* (supplemental Figure 5C) next to Y699, which is crucial for DNA binding and transcriptional activity.[67] *JAK3* mutations occurred at known hotspots reported in T-cell neoplasms with an activating affect.[21,65,68] Five of 6 mutations occurred at hotspot M511I. *JAK2* mutated at a low frequency (2%). Interestingly, I1051T and M1064I were novel mutations. *IL7R* (8%) mutations occurred at the hotspots reported in pediatric T-ALL (supplemental Figure 5D).[66] Reportedly, IL7 signaling induces phosphorylation of *JAK1* and *JAK3*, which in turn phosphorylates *STAT5B*.[69] Notably, cooccurrence of *IL7R* mutations with *NOTCH1* accelerated the development of leukemia in mice.[70] In the current analysis, *STAT5B*^{mut} frequently cooccurred with *NOTCH1*^{mut} (supplemental Figure 6). RAS/MEK/ERK signaling is activated through mutations in *NRAS*, *KRAS*, and *BRAF*.[21] Mutations were identified in these genes in 2% to 7% of cases. In *NRAS* and *KRAS*, the mutations occurred in the hotspots reported in T-ALL and T-LBL.[18,23] Addition, novel mutations, V14L and Y64N, were identified in *KRAS*.

The epigenetic modifiers *SETD1B*, *KMT2C*, *KMT2D*, *DNM2*, and *PHF6* mutated at a frequency of 9% to 17%. Unlike the *KMT2C*^{mut}s, the *KMT2D*^{mut}s were twice as frequent in primary samples from relapse$^+$ cases. Furthermore, *KMT2D*^{mut} rarely cooccurred with *KMT2C*^{mut}. Genes related to transcription and DNA repair included in the panel mutated at a low frequency (2% to 7%). Of the 94% of mutations from the targeting sequencing that displayed VAF <75%, ~6% of mutations displayed VAF >75%. Some of the interesting candidates that displayed VAF >75% were *TP53*, *STAT5B*, *PHF6*, *DDX3X*, *FBXW7*, *CDKN1B*, and *MED12*.

Furthermore, other markers, such as loss of heterozygosity in chromosome 6q (LOH6q; 15%) and incidence of absence of the biallelic TRG deletion (ABD; 23%), which had been reported earlier in T-LBL,[16,17,37] were also analyzed for the extended cohort. Within the LOH6q$^+$ cohort, 8 of 18 LOH6q$^+$ occurred in primary-relapse$^+$ cases and of those, 6 were *NOTCH1*^{wt}. In primary-relapse$^-$ cases, 5 of 10 LOH6q$^+$ were *NOTCH1*^{wt}, whereas the remaining 5 were *NOTCH1*^{mut}, displaying a higher number than previously reported.[17]

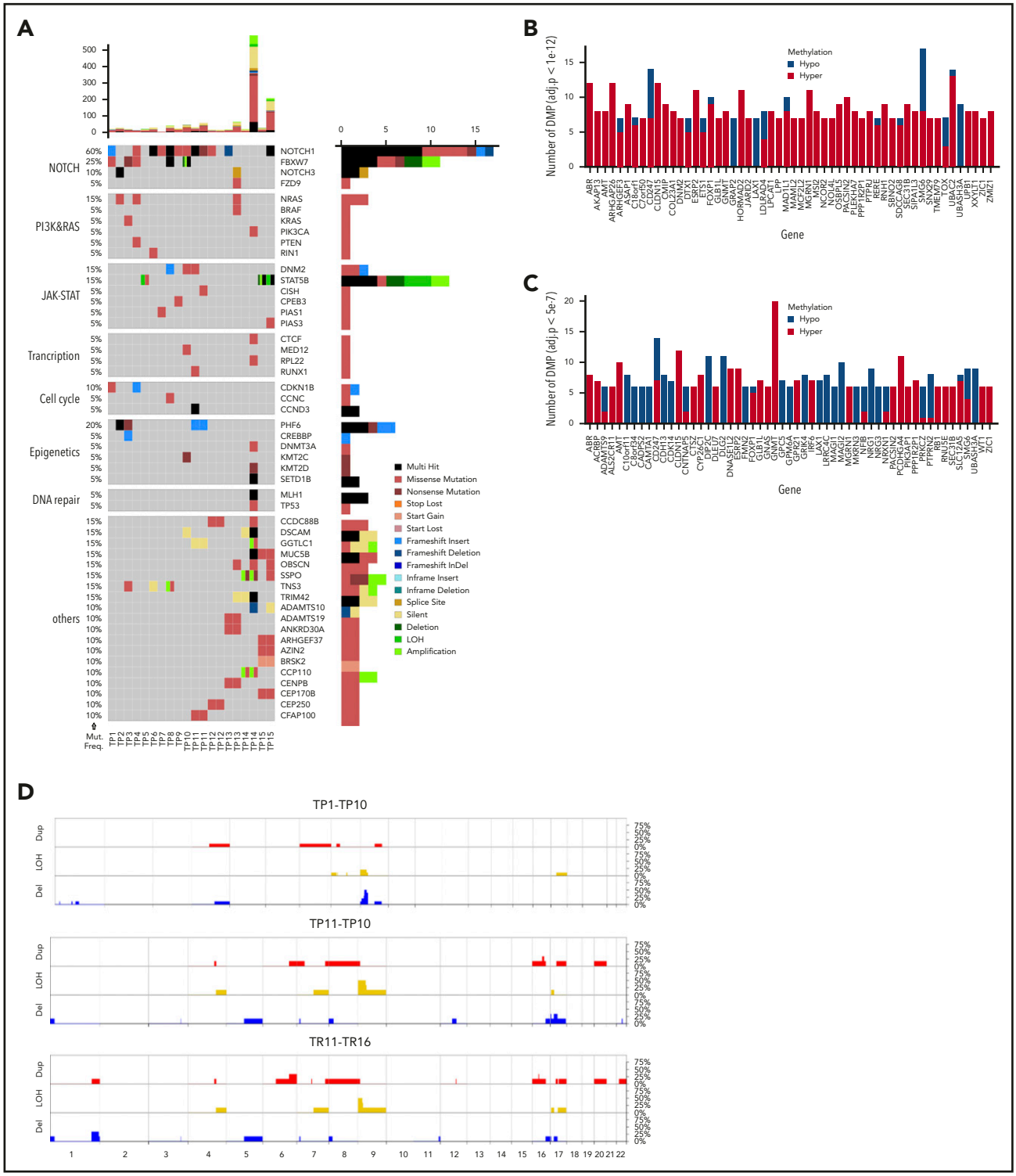

Figure 1. Genome-wide screening for recurrent genetic and epigenetic alterations in T-LBL. (A) Overview of the top 50 mutated genes identified by WES in 15 pediatric T-LBL samples including 5 corresponding relapse samples. The relative mutation frequencies (sample-wise) are indicated to the left and the pathways to the far left. Gene names and types of mutation are to the right. The number of mutations is displayed at the top in a bar plot. (B) The top 55 differentially methylated genes enriched by significant CpGs in primary samples in comparison with their corresponding germline samples (TG vs TP $1e^{-4}$). (C) The top 55 differentially methylated genes enriched by significant CpGs in relapse samples in comparison with their corresponding germline samples (TG vs TR $5e^{-7}$). Array used: Infinium MethylationEPIC BeadChip 850K. (D) The frequency of CNAs detected in 22 T-LBL samples including select primary and matched relapse samples. CNAs in the analyzed samples are displayed against the chromosomal numbers and position. The CNA profiles for primary relapse^{-} samples (TP1-10), for primary relapse^{+} samples (TP11-16), and matched relapse samples (TR11-16) are presented separately. Array used: Infinium Omni2.5Exome-8 v1.3. Results validated independently by MLPA for specific regions in Chr 1p, 4q, 6q, 9p, 10q, 11p, and 17q. Red: amplifications; blue: deletions; yellow: loss of heterozygosity.

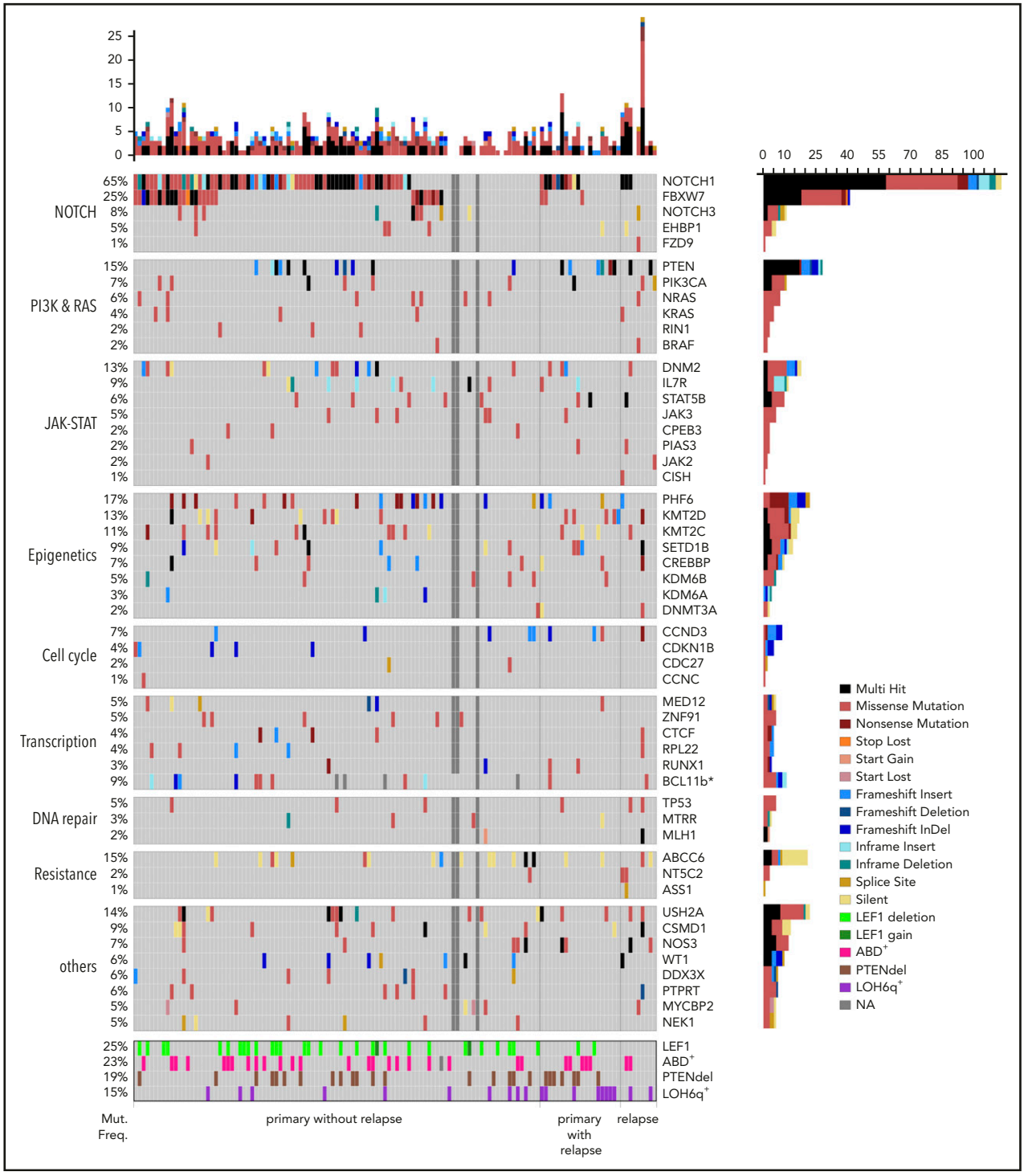

Figure 2. Mutational spectrum of T-LBL. An overview of recurrently mutated genes (VAF cutoff, >10%) and alterations in T-LBL. The samples are sorted into 3 sections: primary samples from relapse^{-} patients, primary samples from relapse^{+} patients, and relapsed cases, as indicated at the bottom of the panel. The frequency of mutations (Mut. Freq.) and name of the pathways is indicated to the left. The names of the genes and the type of mutations are indicated on the right. The number of mutations identified by targeted sequencing is displayed at the top of the plot as bar plots. TRG rearrangements (ABD), *PTEN* deletions (*PTEN*del), and LOH6q alterations are displayed in a subpanel below. **BCL11b* was not part of the targeted panel, but was analyzed by Sanger sequencing. Samples that failed in targeted sequencing are represented in dark gray boxes.

Prognostic relevance of the most significant candidate genes

The clinical characteristics of the patients in the current extended cohort were comparable to those of the cohort in the EURO-LB02 trial, with the exception that a higher proportion of patients in the current analysis were in poor general condition (Table 1).[71]

The results of the current study for the frequency and prognostic relevance of the published markers *NOTCH1* and/or *FBXW7* mutations (*N/F*^{mut}), *PTEN*^{mut}, and LOH6q were consistent, as reported earlier.[1,7,16-18,37,72] *PTEN*^{mut} and LOH6q^{+} were associated with an unfavorable prognosis. Furthermore, ABD^{+} cases were not associated with any outcome in the current analysis,

Table 1. Clinical characteristics of patients from the extended cohort and the trial EURO-LB02

	Targeted sequence (n = 122) n	%	T-LBL cohort from EURO-LB 02 (n = 279) n	%	*P* (targeted cohort vs T-LBL cohort)
Total patients	122		279		
Sex					.5
Male	90	73.8	214	76.7	
Female	32	26.2	65	23.3	
Age, y					.6
<10	64	52.5	154	55.2	
10-14	41	33.6	95	34.1	
≥15	17	13.9	30	10.8	
Stage					.4
II	2	1.8	9	3.9	
III	84	77.1	164	70.7	
IV	23	21.1	59	25.4	
Bone marrow involvement					.9
No	84	80.8	227	81.4	
Yes	20	19.2	52	18.6	
Mediastinal tumor					.2
No	12	9.8	18	6.5	
Yes	110	90.2	261	93.5	
CNS involvement					.1
No	116	98.3	266	95.3	
Yes	2	1.7	13	4.7	
General condition					.03
Good	92	80.7	247	88.8	
Poor (Karnofsky ≤20%)	22	19.3	31	11.2	
Status					
Relapse	20	16.4	34	12.2	

Characteristics of the extended cohort (targeted sequencing) and of the EURO-LB02 trial as the representative reference cohort. All cases for which the corresponding clinical data are available in the NHL-BFM databases are included.

contradicting an earlier report.[16] Intriguingly, *PTEN*del was not associated with an inferior outcome, in contrast to *PTEN*^{mut} (supplemental Figure 7A-F).

The current analysis identified *KMT2D* as a putative novel marker associated with inferior outcomes. *KMT2D* mutations were predominantly localized in 2 hotspots in exons 31 and 48. In primary-relapse^{+} cases and relapse samples, most mutations were identified in exon 48, located before the SET domain (Figure 3). *KMT2D*^{mut} was associated with a significantly higher incidence of relapse compared with *KMT2D*^{mut} (47% ± 17% vs 14% ± 3%; $P = .0064$; Figure 4A). The combination of *KMT2D* and *PTEN* was identified in a subgroup with significantly higher incidence of relapse (Figure 4B). A *KMT2D* and/or a *PTEN* mutation was detected in 27 cases representing 22% of the analyzed cohort. Almost half of all relapses occurred in these 22% of cases. Furthermore, the mutational status of *NOTCH1* and *FBXW7* had significant impact on the prognostic relevance of *KMT2D*^{mut} and/or *PTEN*^{mut} (Figure 4C). Among cases with *NOTCH1*^{wt} and *FBXW7*^{wt}, the relapse incidence was 67% ± 15% in cases with *KMT2D*^{mut} and/or *PTEN*^{mut} status, compared with 11% ± 6% in cases with *KMT2D*^{wt}/*PTEN*^{wt} status ($P < .0001$). Interestingly, *KMT2D*^{mut} (n = 4) and *PTEN*^{mut} (n = 7) in this subgroup did not overlap, except in 1 additional case, suggesting that *KMT2D* and *PTEN* are independent parameters of prognostic relevance (supplemental Table 5). Furthermore, multivariate analysis suggested that, in patients with *NOTCH1*^{wt} and *FBXW7*^{wt}, both *PTEN*^{mut} and *KMT2D*^{mut} are independent parameters that are associated with a higher incidence of relapse (Table 2).

Importantly, in cases with *NOTCH1*^{mut} and/or *FBXW7*^{mut}, when either mutations in the hotspots (Figure 4D) or total mutations were included, the mutational status of *KMT2D* and *PTEN* was of no prognostic relevance. *KMT2C*, another member of Set1/COMPASS-like complexes,[29,73] was not associated with prognostic relevance (supplemental Figure 8A). Mutations in other candidates of interest, such as *NOTCH3*, *PHF6*, *BCL11b*, and *PIK3CA*, as well as deletions in *CDKN2A/CDKN2B*, were not of prognostic relevance. Mutations or deletions in *TP53* were

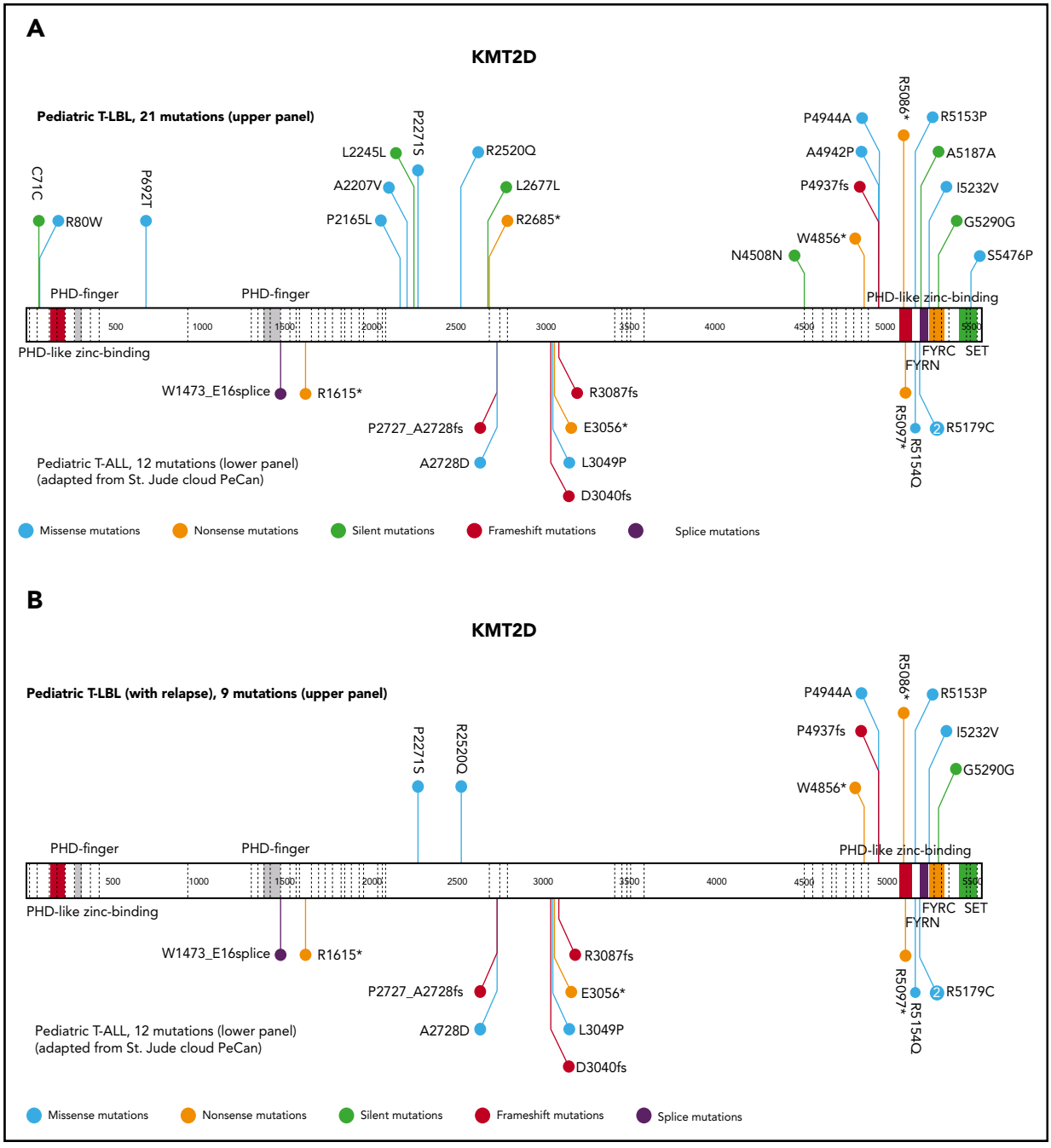

Figure 3. Schematic display of localization and frequencies of mutations in *KMT2D* and prognostic value of the most relevant candidate genes. Schematic display of localization and frequencies of mutations identified for *KMT2D* in total T-LBL samples (VAF cutoff, >1%) (A), *KMT2D* in relapse$^+$ samples (B). The data for mutations (A-B) in pediatric patients with T-ALL were imported from the St Jude Pediatric Cancer Genomic data portal and are displayed in the lower part of the schematic structure, and the mutations identified in the current T-LBL project are displayed in the upper part.

observed in too few cases to draw a conclusion on association with outcome. Deletions in *LEF1* (*LEF1*del) showed a trend toward favorable outcome (supplemental Figure 8B-F).

Impact of the identified mutations on the structure and function of *KMT2D*

KMT2D is a rather large protein (~600 kDa), closely related to *KMT2A*[74] and *KMT2C*.[75] *KMT2D* features 7 PHD fingers, FY-rich domains (FYRN and FYRC), and a highly conserved C-terminal catalytic su(var)3-9, enhancer of zeste, trithorax (SET) domain.[46] The PHD_2 in *KMT2D* has an E3 ligase function similar to the PHD_2 from *MLL1*,[74] PHD_4-PHD_6 was reported to be associated with histone H4,[76] and PHD_6 was shown to have high selectivity for H4K16ac.[77] The PHD_7 and FYR region in *KMT2D* have not been found to be associated with any function. Interestingly, most mutations in *KMT2D* from the relapse$^-$ cases were located in the disordered regions, and, in relapse$^+$ cases, most were located in the ordered regions (Figure 5A). The mutations R5153P, I5232V, and S5476P, identified in T-LBL, and R5154Q, found in pediatric T-ALL, located in the ordered regions, were

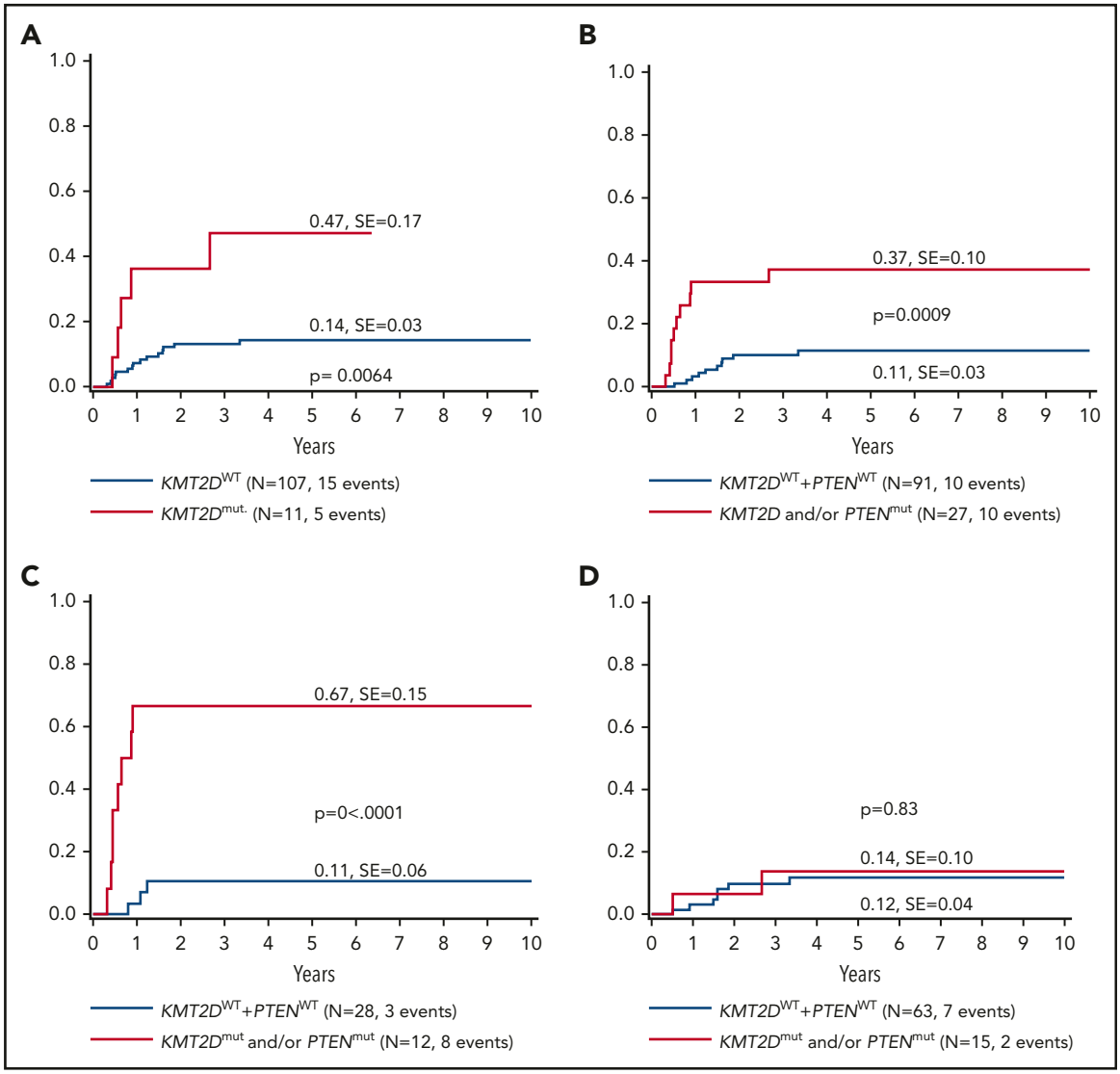

Figure 4. Five-year cumulative incidence of relapse. *KMT2D* mutational status (A), *KMT2D* and *PTEN* mutational status (B), *KMT2D* and *PTEN* mutational status on an *N/F*^{wt} background (C) and *KMT2D* and *PTEN* mutational status on an *N/F*^{mut} background (D). A VAF cutoff of >10% and only nonsynonymous mutations were included for analysis. In case of *N/F*^{mut}, only mutations from the hotspots (exons 26, 27, and 34 for *NOTCH1* and exons 9, 10, and 12 for *FBXW7*) were included.

simulated and modeled to determine their impact on the potential structure and molecular dynamics and their plausible functional impact. An additional mutation, R5179C, has been reported recently in pediatric T-ALL.[78] The modeled structure of PHD_7 revealed an atypical Cys_4-His-Cys_3-His motif. R5153 and R5154 were predicted to be located in a loop structure farther away from the zinc fingers. The R5153P or R5154Q mutations would disrupt interactions with regions of tandem Glu and Asp residues in FYRC domain (supplemental Figure 9A-B; Figure 5B). The FYRN and FYRC motifs are poorly characterized phenylalanine/tyrosine-rich regions common to all KMT2 proteins. The only available crystal structure of FYRN and FYRC motifs is that of the transforming growth factor-β regulator 1 (*TBRG1*) protein.[45] The FYRN and FYRC motifs are adjacent to each other in *KMT2D* and in *KMT2C*, unlike their location in other members of the KMT2 family.[46] To analyze the effect of these newly identified mutations on the FYR motif in *KMT2D*, the crystal structure of the TBRG1 motif was used (PDB: 2WZO). Phyre2 predicted a nearly identical structure via homology modeling, and Ile5232 was located in the core of the hydrophobic pocket. Mutation I5232V led to loss of a CH3 group that normally occupies part of the space in the hydrophobic pocket (Figure 5C-D) and results in destabilization of the domain and causes folding defects.

The crystal structure of the SET domain of *KMT2D*[46] was used to model the S5476P mutation (PDB: 4Z4P). S5476 is located near the *S*-adenosylmethionine (SAM) binding cleft (*S*-adenosyl homocysteine [SAH] is modeled) and makes direct contact with a water molecule that supports Cys5532 (located in a post-SET loop), which is involved in zinc binding (Figure 5E). The S5476P mutation most likely has multiple effects on protein stability. First, the mutation could affect interaction with water binding, destabilizing the Cys-zinc interaction required for folding. In addition, substituting a Pro for a Ser residue may make the loop rigid and reduce the interaction of SAM to the backbones of Asn5474 and His5475 (Figure 5F). In both scenarios, the mutations would affect the function and structure of the protein.

Table 2. Multivariate analysis of the cumulative incidence of relapse using a Fine and Gray model

Parameters	Hazard ratio	95% CI	*P*
FBXW7/NOTCH1	1.2	0.25-5.5	.84
PTEN	1.8	0.20-15.7	.61
KMT2D	1.4	0.17-11.7	.76
LOH6q	3.2	1.0-9.9	.04
Interaction: *NOTCH1* or *FBXW7* with *PTEN*	0.4	0.04-5.7	.53
Interaction: *NOTCH1* or *FBXW7* with *KMT2D*	0.86	0.06-11.8	.90
Interaction: *NOTCH1* or *FBXW7* with *PTEN* or *KMT2D*	13.5	1.1-170.5	.04

In a multivariate analysis with the factors *NOTCH1*^{mut} or *FBXW7*^{mut}, *KMT2D*, *PTEN*, LOH6q mutations and interaction terms between *PTEN*, *KMT2D*, *PTEN* or *KMT2D* and *NOTCH1/FBXW7* (both WT); only LOH6q and the interaction term with *PTEN* or *KMT2D* were significant.

Discussion

The regulation of Notch-mediated transcription depends on the fine balance of the dynamics between the 2 regulatory complexes, namely the NCoR repressive complex and the *KMT2D* activating complex, which compete to bind the SPOC (spen paralogue and ortholog C-terminal) domain of SHARP (SMRT/HDAC1-associated repressor protein).[50,79] The findings from the current analysis suggest that this balance is plausibly disrupted in T-LBL (supplemental Figure 10A), predominantly by *NOTCH1* and *FBXW7* oncogenic alterations that could result in the prolonged activation of NOTCH signaling in >60% of cases in the current analysis and also as reported earlier in T-LBL[1,7,16-18] and T-ALL.[7,9-11,80] Furthermore, somatic mutations and epigenetic modifications, respectively, were identified in the key players *KMT2D* and *NCoR2* of the Notch regulatory network. Hypermethylation of *NCoR2* in primary samples plausibly results in reduced expression of *NCoR2*, affecting the stability of the NCoR repressive complex and providing an additional mechanism that aids in activation of the NOTCH target genes. In contrast, LOF mutations in *KMT2D* could alter the stability of the activator complex (supplemental Figure 10B), thus affecting the expression of tumor-suppressor genes and lineage-specific genes besides the NOTCH target genes. Furthermore, 1 of the downstream targets of hyperactive PI3K-AKT pathway is *KMT2D*. *KMT2D* is phosphorylated by AKT, resulting in attenuation of its methyltransferase activity,[81-83] presumably having an impact similar to that of LOF mutations in *KMT2D*.

Similar to T-ALL, the mutated genes identified in the current analysis could be assigned to the major oncogenic pathways: NOTCH signaling and the PI3K-AKT, Ras, and JAK-STAT pathways, along with cell cycle regulators and epigenetic modifiers. NOTCH signaling (68%) and deletion of the tumor suppressors *p16*^{INK4A} and *p14*^{ARF} encoded in the CDKN2A locus were the most frequent alterations (identified in >70% cases), comparable to previous reports on T-LBL and T-ALL,[26,84] suggesting that deregulation of the cell cycle and prolonged activation of NOTCH signaling are predominantly the key oncogenic events leading to T-cell transformation in both T-ALL and T-LBL. Cross talk between NOTCH signaling and other pathways such as PI3K-AKT, JAK-STAT, and the epigenetic modifier *KMT2D* was suggested by the results of our analysis. In addition, *LEF1*del (23%) was identified. *LEF1* inactivation presumably coordinates with *NOTCH1* activation to activate MYC expression. Interestingly, *LEF1*del showed a trend toward favorable prognosis, as was reported for T-ALL.[85]

N/F^{mut} was associated with a good prognosis for T-LBL, as reported earlier.[1,7,16-18] In the ongoing international clinical trial LBL 2018 (www.clinicaltrials.gov #NCT04043494) with 21 participating countries, the mutational status of *N/F* serves as a stratification criterion. One of the most important translational outcomes of the current study was the observation of the impact of *KMT2D* and *PTEN* mutations. The incidence of relapse for patients with *N/F*^{wt} status was 28% ± 7%. Among the *N/F*^{wt} cohort, 8 of 12 relapses occurred in the patients with *PTEN* and/or *KMT2D* mutations. Multivariate analysis suggested that, in patients with wild-type *NOTCH1* and *FBXW7*, the independent prognostic parameters *PTEN* or *KMT2D* are associated with a higher incidence of relapse. Interestingly, in the *N/F*^{mut} cohort, the mutational status of *KMT2D* and *PTEN* did not have any prognostic relevance.

Furthermore, investigations were conducted into the effect of mutations on the individual domains of *KMT2D*. FYRN and FYRC motifs are thought to play a role in chromatin binding[45]; identified mutations in this region may affect the binding of *KMT2D* to its target genes. PHD domains in *KMT2C/KMT2D* have been reported to play an important role in homodimerization, recruitment of *KMT2C/KMT2D* complexes to their target genes, and methylation.[75] *KMT2D* protein stability is tightly regulated by its H3K4 methyltransferase activity; mutations in the SET domain results in enzymatically dead *KMT2D*.[86] Hence, the mutations identified in cases of T-LBL relapse may cause truncation leading to loss of the SET domain, resulting in enzymatically dead protein affecting expression of some of the target genes. Very little is known about *KMT2D* mutations in T-ALL, no association with prognostic relevance has been reported so far.[21,22] In a mouse model, ablation of *KMT2D* in B cells promoted lymphoma, and brain-specific knockout of *KMT2D* induced medulloblastoma.[32,87] Interestingly, its paralogue, *KMT2C*,[88] was not associated with prognostic relevance in the current analysis, suggesting a diverse and nonredundant role of *KMT2D* in T-LBL. These results certainly require validation in larger and prospective cohorts, which will be achieved by the molecular analyses of patients enrolled in the LBL 2018 trial.

In contrast to T-ALL, 2 aspects are highly relevant to the interpretation and consequences of our current results. First, the treatment regimen for T-LBL, based on the EURO-LB02 trial, was internationally uniform.[71] Second, no stratification criteria were applied for intensification of treatment of the analyzed cohort. These factors resulted in uniform treatment of the patients with T-LBL in the current study and sets a strong basis for translational research aimed at identifying molecular markers with prognostic relevance.

Similar to observations in T-ALL,[21] only *NOTCH1* and *CDKN2A/B* were mutated or deleted in >60% of the cases, whereas most

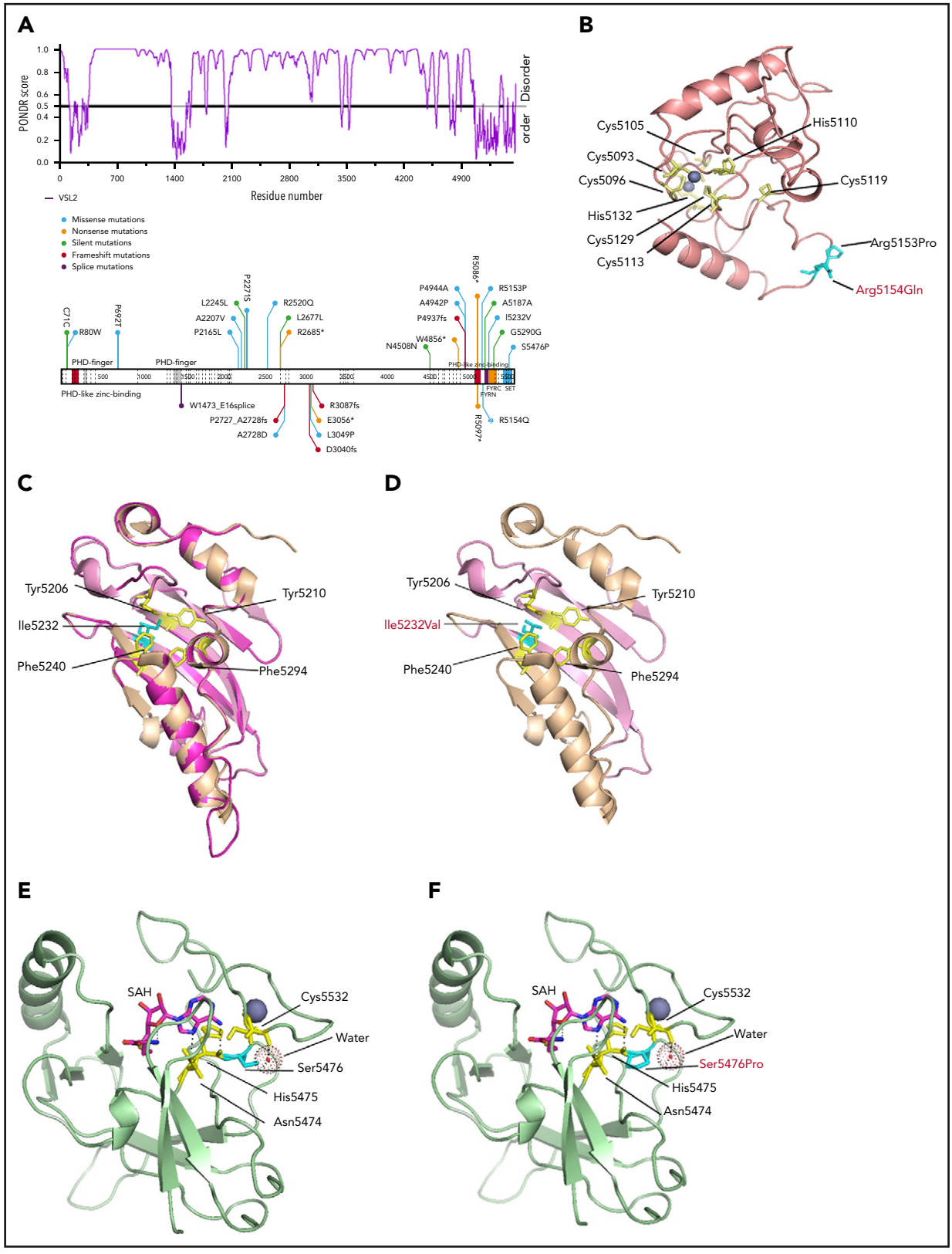

Figure 5. Modeling of *KMT2D* domain structures and comparison with the mutated domain structures. (A) Schematic overview of the predictive value of intrinsically disordered regions in *KMT2D*. The KMT2D gene is aligned with the PONDR (Predictor of Naturally Disordered Regions) chart to visualize mutations that lie in the predicted disordered region. (B) The domain structure of PHD_7 of $KMT2D^{wt}$ was generated by Phyre2. The schematic display of Arg residues (cyan) are represented in the stick structures near PHD_7 of $KMT2D^{mut}$ at the respective positions R5153P and R5154Q (cyan), the latter having been identified in T-ALL (red). (C) The crystal structure of the FYR domain, superimposition of Phyre2 depiction of the *KMT2D* (magenta), FYRN (pink), and FYRC (orange) motifs with the crystal structure of the *TBRG1* motif (PDB: 2WZO).[45] The residues forming the core hydrophobic pocket (yellow) are shown with stick structures and display of the Ileu5232 (cyan) in the FYRN motif. (D) The mutation Ileu5232Val (cyan) leads to loss of CH3, which could result in destabilizing of the domain. (E) Crystal structure of *KMT2D* SET domain (PDB: 4Z4P).[46] The mutation Ser5476 (cyan) is located near the SAM binding cleft (SAH is modeled) and makes direct contact with a water molecule that supports Cys5532 (yellow, stick structure) located in the post-SET loop involved in zinc binding (purple). (F) The Ser5476Pro mutation impairs water binding, which could destabilize the Cys-zinc interaction required for proper folding.

of the genes analyzed were mutated in <10% of cases, suggesting the complexity and heterogeneity of events underlying the malignant transformation of T-LBL. Some of the limitations of this study were that the methylation arrays were performed only for the limited cohort and that 1 (TP79) of 122 analyzed cases did not feature any somatic mutations in the genes included in the targeted panel or other markers included in the study, suggesting the need to perform genome-wide analysis on larger cohorts to identify additional candidate genes and/or epigenetic alterations relevant to T-LBL.

Acknowledgments

The authors thank the participating centers of the NHL-BFM Group that provided samples and clinical information; Harshana Sabharwal for technical help in preparing the samples for targeted sequencing; the members of the NHL-BFM study center in Muenster for feedback and constant help in organizing data and patient samples; and the family of Jonas Goeckener for their contribution, which was helpful in the preliminary experiments.

This work was supported by Deutsche Krebshilfe (DKH) grant 111347 (B.B., M.D.).

Authorship

Contribution: B.B., T.K., M.D., and M.Z. conceptualized and designed the project. B.B., S.M., H.H., I.O., W.K., and W.W. organized the patient and study material; T.K., S.S., J.S., C.R., M.Z., C.B., G.R., S.M., H.H., C.W., I.O., W.K., M.D., and B.B. collected and assembled the data; T.K., B.B., S.S., M.D., M.Z., J.S., C.R., M.Z., C.B., A.B.N., H.G., P.H., S.H., L.W., W.W., M.W., and M.D. analyzed and interpreted the data; T.K., B.B., S.S., M.D., H.G., and M.Z. wrote the manuscript; and all authors read and approved the manuscript.

Conflict-of-interest disclosure: The authors declare no competing financial interests.

ORCID profiles: S.S., 0000-0002-5011-0641; A.B.N., 0000-0001-8551-0269; S.H., 0000-0002-2786-8200; C.W., 0000-0003-4367-3857; H.G., 0000-0002-1250-9571; W.K., 0000-0001-7208-4117; M.D., 0000-0001-9740-0788; B.B., 0000-0002-1151-829X.

Correspondence: Birgit Burkhardt, Pediatric Hematology and Oncology, University Hospital Muenster, 48149 Muenster, Germany; e-mail: birgit.burkhardt@ukmuenster.de.

Footnotes

Submitted 18 February 2020; accepted 14 October 2020; prepublished online on *Blood* First Edition 5 November 2020. DOI 10.1182/blood.2020005381.

The WES and targeted sequencing data for this study have been deposited in the European Nucleotide Archive (ENA) at EMBL-EBI under accession number PRJEB36436 (https://www.ebi.ac.uk/ena/data/view/PRJEB36436). The methylation array has been deposited in the ArrayExpress database at EMBL-EBI under accession number E-MTAB-8762 (https://www.ebi.ac.uk/arrayexpress/experiments/E-MTAB-8762). SNP array data have been deposited in the ArrayExpress database at EMBL-EBI under accession number E-MTAB-8763 (https://www.ebi.ac.uk/arrayexpress/experiments/E-MTAB-8763).

The online version of this article contains a data supplement.

There is a *Blood* Commentary on this article in this issue.

The publication costs of this article were defrayed in part by page charge payment. Therefore, and solely to indicate this fact, this article is hereby marked "advertisement" in accordance with 18 USC section 1734.

REFERENCES

1. Basso K, Mussolin L, Lettieri A, et al. T-cell lymphoblastic lymphoma shows differences and similarities with T-cell acute lymphoblastic leukemia by genomic and gene expression analyses. *Genes Chromosomes Cancer*. 2011;50(12):1063-1075.

2. Raetz EA, Perkins SL, Bhojwani D, et al. Gene expression profiling reveals intrinsic differences between T-cell acute lymphoblastic leukemia and T-cell lymphoblastic lymphoma. *Pediatr Blood Cancer*. 2006;47(2):130-140.

3. Burkhardt B. Paediatric lymphoblastic T-cell leukaemia and lymphoma: one or two diseases? *Br J Haematol*. 2010;149(5):653-668.

4. Van Vlierberghe P, Ferrando A. The molecular basis of T cell acute lymphoblastic leukemia. *J Clin Invest*. 2012;122(10):3398-3406.

5. Weng AP, Ferrando AA, Lee W, et al. Activating mutations of NOTCH1 in human T cell acute lymphoblastic leukemia. *Science*. 2004;306(5694):269-271.

6. Breit S, Stanulla M, Flohr T, et al. Activating NOTCH1 mutations predict favorable early treatment response and long-term outcome in childhood precursor T-cell lymphoblastic leukemia. *Blood*. 2006;108(4):1151-1157.

7. Park MJ, Taki T, Oda M, et al. FBXW7 and NOTCH1 mutations in childhood T cell acute lymphoblastic leukaemia and T cell non-Hodgkin lymphoma. *Br J Haematol*. 2009;145(2):198-206.

8. Larson Gedman A, Chen Q, Kugel Desmoulin S, et al. The impact of NOTCH1, FBW7 and PTEN mutations on prognosis and downstream signaling in pediatric T-cell acute lymphoblastic leukemia: a report from the Children's Oncology Group. *Leukemia*. 2009;23(8):1417-1425.

9. Clappier E, Collette S, Grardel N, et al; EORTC-CLG. NOTCH1 and FBXW7 mutations have a favorable impact on early response to treatment, but not on outcome, in children with T-cell acute lymphoblastic leukemia (T-ALL) treated on EORTC trials 58881 and 58951. *Leukemia*. 2010;24(12):2023-2031.

10. Zuurbier L, Homminga I, Calvert V, et al. NOTCH1 and/or FBXW7 mutations predict for initial good prednisone response but not for improved outcome in pediatric T-cell acute lymphoblastic leukemia patients treated on DCOG or COALL protocols. *Leukemia*. 2010;24(12):2014-2022.

11. Kox C, Zimmermann M, Stanulla M, et al. The favorable effect of activating NOTCH1 receptor mutations on long-term outcome in T-ALL patients treated on the ALL-BFM 2000 protocol can be separated from FBXW7 loss of function. *Leukemia*. 2010;24(12):2005-2013.

12. Erbilgin Y, Sayitoglu M, Hatirnaz O, et al. Prognostic significance of NOTCH1 and FBXW7 mutations in pediatric T-ALL. *Dis Markers*. 2010;28(6):353-360.

13. Mansur MB, Hassan R, Barbosa TC, et al. Impact of complex NOTCH1 mutations on survival in paediatric T-cell leukaemia. *BMC Cancer*. 2012;12(1):9.

14. Jenkinson S, Koo K, Mansour MR, et al. Impact of NOTCH1/FBXW7 mutations on outcome in pediatric T-cell acute lymphoblastic leukemia patients treated on the MRC UKALL 2003 trial. *Leukemia*. 2013;27(1):41-47.

15. Kimura S, Seki M, Yoshida K, et al. NOTCH1 pathway activating mutations and clonal evolution in pediatric T-cell acute lymphoblastic leukemia. *Cancer Sci*. 2019;110(2):784-794.

16. Callens C, Baleydier F, Lengline E, et al. Clinical impact of NOTCH1 and/or FBXW7 mutations, FLASH deletion, and TCR status in pediatric T-cell lymphoblastic lymphoma. *J Clin Oncol*. 2012;30(16):1966-1973.

17. Bonn BR, Rohde M, Zimmermann M, et al. Incidence and prognostic relevance of genetic variations in T-cell lymphoblastic lymphoma in childhood and adolescence. *Blood*. 2013;121(16):3153-3160.

18. Balbach ST, Makarova O, Bonn BR, et al. Proposal of a genetic classifier for risk group stratification in pediatric T-cell lymphoblastic lymphoma reveals differences from adult T-cell lymphoblastic leukemia. *Leukemia*. 2016;30(4):970-973.

19. Palomero T, Sulis ML, Cortina M, et al. Mutational loss of PTEN induces resistance to NOTCH1 inhibition in T-cell leukemia. *Nat Med*. 2007;13(10):1203-1210.

20. Palomero T, Dominguez M, Ferrando AA. The role of the PTEN/AKT Pathway in NOTCH1-induced leukemia. *Cell Cycle*. 2008;7(8):965-970.

21. Liu Y, Easton J, Shao Y, et al. The genomic landscape of pediatric and young adult T-lineage acute lymphoblastic leukemia. *Nat Genet*. 2017;49(8):1211-1218.

22. Lindqvist CM, Nordlund J, Ekman D, et al. The mutational landscape in pediatric acute lymphoblastic leukemia deciphered by whole genome sequencing. *Hum Mutat*. 2015;36(1):118-128.

23. Ma X, Liu Y, Liu Y, et al. Pan-cancer genome and transcriptome analyses of 1,699 paediatric leukaemias and solid tumours. *Nature*. 2018;555(7696):371-376.

24. Van Vlierberghe P, Ambesi-Impiombato A, De Keersmaecker K, et al. Prognostic relevance of integrated genetic profiling in adult T-cell acute lymphoblastic leukemia. *Blood*. 2013;122(1):74-82.

25. Gutierrez A, Kentsis A, Sanda T, et al. The BCL11B tumor suppressor is mutated across the major molecular subtypes of T-cell acute lymphoblastic leukemia. *Blood*. 2011;118(15):4169-4173.

26. Krieger D, Moericke A, Oschlies I, et al. Frequency and clinical relevance of DNA microsatellite alterations of the CDKN2A/B, ATM and p53 gene loci: a comparison between pediatric precursor T-cell lymphoblastic lymphoma and T-cell lymphoblastic leukemia. *Haematologica*. 2010;95(1):158-162.

27. Zhang JA, Mortazavi A, Williams BA, Wold BJ, Rothenberg EV. Dynamic transformations of genome-wide epigenetic marking and transcriptional control establish T cell identity. *Cell*. 2012;149(2):467-482.

28. Morin RD, Johnson NA, Severson TM, et al. Somatic mutations altering EZH2 (Tyr641) in follicular and diffuse large B-cell lymphomas of germinal-center origin. *Nat Genet*. 2010;42(2):181-185.

29. Ford DJ, Dingwall AK. The cancer COMPASS: navigating the functions of MLL complexes in cancer [published correction appears in *Cancer Genet*. 2019;233-234:102]. *Cancer Genet*. 2015;208(5):178-191.

30. Ferrero S, Rossi D, Rinaldi A, et al. *KMT2D* mutations and *TP53* disruptions are poor prognostic biomarkers in mantle cell lymphoma receiving high-dose therapy: a FIL study. *Haematologica*. 2020;105(6):1604-1612.

31. Wang H, Zang C, Taing L, et al. NOTCH1-RBPJ complexes drive target gene expression through dynamic interactions with super-enhancers. *Proc Natl Acad Sci USA*. 2014;111(2):705-710.

32. Dhar SS, Zhao D, Lin T, et al. MLL4 Is Required to Maintain Broad H3K4me3 Peaks and Super-Enhancers at Tumor Suppressor Genes. *Mol Cell*. 2018;70(5):825-841 e826.

33. Hu D, Gao X, Morgan MA, Herz HM, Smith ER, Shilatifard A. The MLL3/MLL4 branches of the COMPASS family function as major histone H3K4 monomethylases at enhancers. *Mol Cell Biol*. 2013;33(23):4745-4754.

34. Bonn BR, Huge A, Rohde M, et al. Whole exome sequencing hints at a unique mutational profile of paediatric T-cell lymphoblastic lymphoma. *Br J Haematol*. 2015;168(2):308-313.

35. Li Z, Song Y, Zhang Y, et al. Genomic and outcome analysis of adult T-cell lymphoblastic lymphoma. *Haematologica*. 2020;105(3):e107-e110.

36. Haider Z, Landfors M, Golovleva I, et al. DNA methylation and copy number variation profiling of T-cell lymphoblastic leukemia and lymphoma. *Blood Cancer J*. 2020;10(4):45.

37. Burkhardt B, Bruch J, Zimmermann M, et al. Loss of heterozygosity on chromosome 6q14-q24 is associated with poor outcome in children and adolescents with T-cell lymphoblastic lymphoma. *Leukemia*. 2006;20(8):1422-1429.

38. Reiter A, Schrappe M, Ludwig WD, et al. Intensive ALL-type therapy without local radiotherapy provides a 90% event-free survival for children with T-cell lymphoblastic lymphoma: a BFM group report. *Blood*. 2000;95(2):416-421.

39. Zhou W, Laird PW, Shen H. Comprehensive characterization, annotation and innovative use of Infinium DNA methylation BeadChip probes. *Nucleic Acids Res*. 2017;45(4):e22.

40. Rohde M, Bonn BR, Zimmermann M, et al. Multiplex ligation-dependent probe amplification validates LOH6q analyses and enhances insight into chromosome 6q aberrations in pediatric T-cell lymphoblastic leukemia and lymphoma. *Leuk Lymphoma*. 2015;56(6):1884-1887.

41. Derrieux C, Trinquand A, Bruneau J, et al. A Single-Tube, EuroClonality-Inspired, TRG Clonality Multiplex PCR Aids Management of Patients with Enteropathic Diseases, including from Formaldehyde-Fixed, Paraffin-Embedded Tissues. *J Mol Diagn*. 2019;21(1):111-122.

42. Fine JP, Gray RJ. A Proportional Hazards Model for the Subdistribution of a Competing Risk. *J Am Stat Assoc*. 1999;94(446):496-509.

43. Peng K, Radivojac P, Vucetic S, Dunker AK, Obradovic Z. Length-dependent prediction of protein intrinsic disorder. *BMC Bioinformatics*. 2006;7(1):208.

44. Kelley LA, Mezulis S, Yates CM, Wass MN, Sternberg MJE. The Phyre2 web portal for protein modeling, prediction and analysis. *Nat Protoc*. 2015;10(6):845-858.

45. García-Alai MM, Allen MD, Joerger AC, Bycroft M. The structure of the FYR domain of transforming growth factor beta regulator 1. *Protein Sci*. 2010;19(7):1432-1438.

46. Zhang Y, Mittal A, Reid J, Reich S, Gamblin SJ, Wilson JR. Evolving Catalytic Properties of the MLL Family SET Domain. *Structure*. 2015;23(10):1921-1933.

47. Johnson A, Severson E, Gay L, et al. Comprehensive Genomic Profiling of 282 Pediatric Low- and High-Grade Gliomas Reveals Genomic Drivers, Tumor Mutational Burden, and Hypermutation Signatures. *Oncologist*. 2017;22(12):1478-1490.

48. Lawrence MS, Stojanov P, Polak P, et al. Mutational heterogeneity in cancer and the search for new cancer-associated genes. *Nature*. 2013;499(7457):214-218.

49. Huang W, Sherman BT, Lempicki RA. Bioinformatics enrichment tools: paths toward the comprehensive functional analysis of large gene lists. *Nucleic Acids Res*. 2009;37(1):1-13.

50. Oswald F, Rodriguez P, Giaimo BD, et al. A phospho-dependent mechanism involving NCoR and KMT2D controls a permissive chromatin state at Notch target genes. *Nucleic Acids Res*. 2016;44(10):4703-4720.

51. Feng X, Ippolito GC, Tian L, et al. Foxp1 is an essential transcriptional regulator for the generation of quiescent naive T cells during thymocyte development. *Blood*. 2010;115(3):510-518.

52. Shahryari A, Jazi MS, Samaei NM, Mowla SJ. Long non-coding RNA SOX2OT: expression signature, splicing patterns, and emerging roles in pluripotency and tumorigenesis. *Front Genet*. 2015;6:196.

53. Yang L, Li Y, Bhattacharya A, Zhang Y. PEPD is a pivotal regulator of p53 tumor suppressor. *Nat Commun*. 2017;8(1):2052.

54. Shan J, Liu Y, Wang Y, Li Y, Yu X, Wu C. GALNT14 Involves the Regulation of Multidrug Resistance in Breast Cancer Cells. *Transl Oncol*. 2018;11(3):786-793.

55. O'Neil J, Grim J, Strack P, et al. FBW7 mutations in leukemic cells mediate NOTCH pathway activation and resistance to gamma-secretase inhibitors. *J Exp Med*. 2007;204(8):1813-1824.

56. Silva A, Yunes JA, Cardoso BA, et al. PTEN posttranslational inactivation and hyperactivation of the PI3K/Akt pathway sustain primary T cell leukemia viability. *J Clin Invest*. 2008;118(11):3762-3774.

57. Shan X, Czar MJ, Bunnell SC, et al. Deficiency of PTEN in Jurkat T cells causes constitutive localization of Itk to the plasma membrane and hyperresponsiveness to CD3 stimulation. *Mol Cell Biol*. 2000;20(18):6945-6957.

58. Zuurbier L, Petricoin EF III, Vuerhard MJ, et al. The significance of PTEN and AKT aberrations in pediatric T-cell acute lymphoblastic leukemia. *Haematologica*. 2012;97(9):1405-1413.

59. Bandapalli OR, Schuessele S, Kunz JB, et al. The activating STAT5B N642H mutation is a common abnormality in pediatric T-cell acute lymphoblastic leukemia and confers a higher risk of relapse. *Haematologica*. 2014;99(10):e188-e192.

60. Zhang W, Liang X, Gong Y, Xiao C, Guo B, Yang T. The Signal Transducer and Activator of Transcription 5B (STAT5B) Gene Promotes Proliferation and Drug Resistance of Human Mantle Cell Lymphoma Cells by Activating the Akt Signaling Pathway. *Med Sci Monit*. 2019;25:2599-2608.

61. Küçük C, Jiang B, Hu X, et al. Activating mutations of STAT5B and STAT3 in lymphomas derived from γδ-T or NK cells. *Nat Commun*. 2015;6(1):6025.

62. Kontro M, Kuusanmäki H, Eldfors S, et al. Novel activating STAT5B mutations as putative drivers of T-cell acute lymphoblastic leukemia. *Leukemia*. 2014;28(8):1738-1742.

63. Gouilleux-Gruart V, Gouilleux F, Desaint C, et al. STAT-related transcription factors are constitutively activated in peripheral blood cells from acute leukemia patients. *Blood*. 1996;87(5):1692-1697.

64. Zhang Q, Nowak I, Vonderheid EC, et al. Activation of Jak/STAT proteins involved in signal transduction pathway mediated by receptor for interleukin 2 in malignant T lymphocytes derived from cutaneous anaplastic large T-cell lymphoma and Sezary syndrome. *Proc Natl Acad Sci USA*. 1996;93(17):9148-9153.

65. Greenplate A, Wang K, Tripathi RM, et al. Genomic profiling of T-cell neoplasms reveals frequent JAK1 and JAK3 mutations with clonal evasion from targeted therapies. *JCO Precis Oncol*. 2018;PO.17.00019.

66. Li Y, Buijs-Gladdines JG, Canté-Barrett K, et al. IL-7 Receptor Mutations and Steroid Resistance in Pediatric T cell Acute Lymphoblastic Leukemia: A Genome Sequencing Study. *PLoS Med*. 2016;13(12):e1002200.

67. Lin JX, Mietz J, Modi WS, John S, Leonard WJ. Cloning of human Stat5B. Reconstitution of interleukin-2-induced Stat5A and Stat5B DNA binding activity in COS-7 cells. *J Biol Chem*. 1996;271(18):10738-10744.

68. Gröbner SN, Worst BC, Weischenfeldt J, et al; ICGC MMML-Seq Project. The landscape of genomic alterations across childhood cancers. *Nature*. 2018;555(7696):321-327.

69. Vainchenker W, Constantinescu SN. JAK/STAT signaling in hematological malignancies. *Oncogene*. 2013;32(21):2601-2613.

70. Yokoyama K, Yokoyama N, Izawa K, et al. In vivo leukemogenic potential of an interleukin 7 receptor α chain mutant in hematopoietic stem and progenitor cells. *Blood*. 2013;122(26):4259-4263.

71. Landmann E, Burkhardt B, Zimmermann M, et al. Results and conclusions of the European Intergroup EURO-LB02 trial in children and adolescents with lymphoblastic lymphoma. *Haematologica*. 2017;102(12):2086-2096.

72. Baleydier F, Decouvelaere AV, Bergeron J, et al. T cell receptor genotyping and HOXA/TLX1 expression define three T lymphoblastic lymphoma subsets which might affect clinical outcome. *Clin Cancer Res*. 2008;14(3):692-700.

73. Rao RC, Dou Y. Hijacked in cancer: the KMT2 (MLL) family of methyltransferases. *Nat Rev Cancer*. 2015;15(6):334-346.

74. Wang J, Muntean AG, Wu L, Hess JL. A subset of mixed lineage leukemia proteins has plant homeodomain (PHD)-mediated E3 ligase activity. *J Biol Chem*. 2012;287(52):43410-43416.

75. Liu Y, Qin S, Chen TY, et al. Structural insights into trans-histone regulation of H3K4 methylation by unique histone H4 binding of MLL3/4. *Nat Commun*. 2019;10(1):36.

76. Dhar SS, Lee SH, Kan PY, et al. Trans-tail regulation of MLL4-catalyzed H3K4 methylation by H4R3 symmetric dimethylation is mediated by a tandem PHD of MLL4. *Genes Dev*. 2012;26(24):2749-2762.

77. Zhang Y, Jang Y, Lee JE, et al. Selective binding of the PHD6 finger of MLL4 to histone H4K16ac links MLL4 and MOF. *Nat Commun*. 2019;10(1):2314.

78. Li B, Brady SW, Ma X, et al. Therapy-induced mutations drive the genomic landscape of relapsed acute lymphoblastic leukemia. *Blood*. 2020;135(1):41-55.

79. Giaimo BD, Oswald F, Borggrefe T. Dynamic chromatin regulation at Notch target genes. *Transcription*. 2017;8(1):61-66.

80. Ma J, Wu M. The indicative effect of Notch1 expression for the prognosis of T-cell acute lymphocytic leukemia: a systematic review. *Mol Biol Rep*. 2012;39(5):6095-6100.

81. Lv S, Ji L, Chen B, et al. Histone methyltransferase KMT2D sustains prostate carcinogenesis and metastasis via epigenetically activating LIFR and KLF4. *Oncogene*. 2018;37(10):1354-1368.

82. Toska E, Osmanbeyoglu HU, Castel P, et al. PI3K pathway regulates ER-dependent transcription in breast cancer through the epigenetic regulator KMT2D. *Science*. 2017;355(6331):1324-1330.

83. Toska E, Castel P, Chhangawala S, et al. PI3K Inhibition Activates SGK1 via a Feedback Loop to Promote Chromatin-Based Regulation of ER-Dependent Gene Expression. *Cell Rep*. 2019;27(1):294-306 e295.

84. Ferrando AA, Neuberg DS, Staunton J, et al. Gene expression signatures define novel oncogenic pathways in T cell acute lymphoblastic leukemia. *Cancer Cell*. 2002;1(1):75-87.

85. Gutierrez A, Sanda T, Ma W, et al. Inactivation of LEF1 in T-cell acute lymphoblastic leukemia. *Blood*. 2010;115(14):2845-2851.

86. Jang Y, Wang C, Zhuang L, Liu C, Ge K. H3K4 Methyltransferase Activity Is Required for MLL4 Protein Stability. *J Mol Biol*. 2017;429(13):2046-2054.

87. Zhang J, Dominguez-Sola D, Hussein S, et al. Disruption of KMT2D perturbs germinal center B cell development and promotes lymphomagenesis. *Nat Med*. 2015;21(10):1190-1198.

88. Fagan RJ, Dingwall AK. COMPASS Ascending: Emerging clues regarding the roles of MLL3/KMT2C and MLL2/KMT2D proteins in cancer. *Cancer Lett*. 2019;458:56-65.